J. Am. Chem. Soc. 1992, 114, 5585-5590

Probing the Anomeric Effect in Orthoesters. Structure, Conformation, and Dynamic Behavior of a Unique Orthooxalate: 2,5,7,10,11,14-Hexaoxa[4.4.4]propellane[1]

Pinchas Aped, Benzion Fuchs,* Israel Goldberg,* Hanoch Senderowitz, Evgeny Tartakovsky, and Sarah Weinman

Contribution from the School of Chemistry,† Tel-Aviv University, Ramat-Aviv, 69978 Tel-Aviv, Israel. *Received October 9, 1991. Revised Manuscript Received February 27, 1992*

Abstract: Geometrical parameters in the $C(OC)_3$ moiety of a series of orthoesters in X-ray diffraction structures were retrieved from the Cambridge Structural Database (CSD) and analyzed in the context of stereoelectronic effects. The seven independent conformers of trimethyl orthoformate (3) were calculated both ab initio, using the 3-21G basis set, and with the MM2 force field suitably parametrized to include structural manifestations of the anomeric effect (MM2-AE). Selected orthoesters were calculated using this force field, and good agreement was obtained. The structure and conformation of the title compound HOP (4), a unique D_3 orthooxalate, were investigated. The geometrical parameters of the anomeric moieties and the ring conformation were scrutinized in the crystal using X-ray diffraction analysis and by MM2-AE computation: very good agreement between the two methods was obtained. The kinetics of the ring-inversion (enantiomer interconversion) process of the system were interrogated in a variable temperature ^{1}H-NMR spectroscopic study of HOP-d_{11}, yielding $\Delta G^{\ddagger} = 11.8$ kcal/mol. This result is discussed in the framework of a MM3 computational study of the minima and transition states encountered in the inversion process of HOP.

Introduction

In the framework of our studies on saturated polyheterocycles with stereoelectronic effects, we have studied some time ago *cis*-1,4,5,8-tetraoxadecalin (1, X = H)[2] and its substituted derivatives,[3,4] as well as various aspects of the *anomeric effect*[5] in O–C–O-containing systems.[6-8] In the course of these efforts, we have reparametrized the MM2 force field[10,11] to account for the structural manifestations of the anomeric effect (MM2-AE).[7,17] Earlier, we had also described[3c,9] the preparation and properties of various 9,10-annelated *cis*-1,4,5,8-tetraoxadecalins (2) (i.e., 2,5,7,10-tetraoxa[*n*.4.4]propellanes), and recently[1] we investigated the structure and conformation of a series of such interesting compounds.

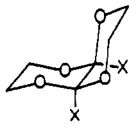

1

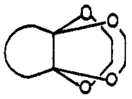

2

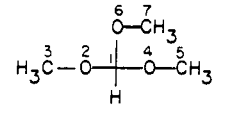

$H_3C{-}O{-}\overset{\displaystyle O{-}CH_3}{\underset{\displaystyle H}{C}}{-}O{-}CH_3$

3

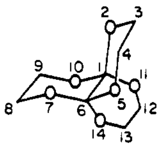

4

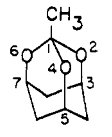

5

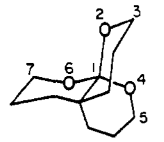

6

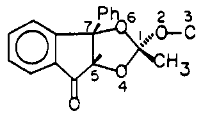

7

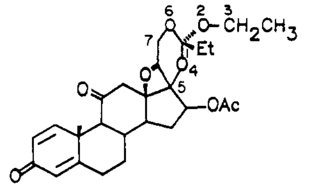

8

Results and Discussion

As a sequel to the above, we focused our attention on a group of compounds featuring overlapping anomeric COCOC units, namely, orthoesters. The seven independent, nondegenerate *ideal* conformations of the smallest prototype, trimethyl orthoformate

---

† The School of Chemistry at Tel-Aviv University is part of the Raymond and Beverly Sackler Faculty of Exact Sciences.

[1] Structure and Conformation of Heterocycles. 21. Part 20: Aped, P.; Fuchs, B.; Goldberg, I.; Senderowitz, H.; Schleifer, L.; Tartakovsky, E.; Anteunis, M.; Borremans, F. *Tetrahedron* **1991**, *47*, 5781.

[2] Goldberg, I.; Shmueli, U.; Fuchs, B. *J. Chem. Soc., Perkin Trans. 2* **1972**, 357.

[3] (a) Fuchs, B. *Tetrahedron Lett.* **1969**, 3571. (b) Fuchs, B. *Tetrahedron Lett.* **1970**, 1747. (c) Erez, M.; Fuchs, B. *Tetrahedron Lett.* **1971**, 4931.

[4] (a) Fuchs, B.; Auerbach, Y.; Sprecher, M. *Tetrahedron* **1974**, *30*, 437. (b) Fuchs, B.; Auerbach, Y.; Sprecher, M. *Tetrahedron Lett.* **1970**, 5207.

[5] (a) Szarek, W. A., Horton, D., Eds. *Anomeric Effect. Origin and Consequences* ACS Monograph Series; American Chemical Society: Washington, DC, 1979; Vol. 87. (b) Kirby, A. J. *The Anomeric Effect and Related Stereoelectronic Effects at Oxygen*; Springer: Berlin, 1983. (c) Deslongchamps, P. *Stereoelectronic Effects in Organic Chemistry*; Wiley: New York, 1983.

[6] Fuchs, B.; Ellencweig, A.; Tartakovsky, E., Aped, P. *Angew. Chem., Int. Ed. Engl.* **1986**, *25*, 287.

[7] Aped, P.; Apeloig, Y.; Ellencweig, A.; Fuchs, B.; Goldberg, I.; Karni, M.; Tartakovsky, E. *J. Am. Chem. Soc.* **1987**, *109*, 1486.

[8] (a) Schleifer, L.; Senderowitz, H.; Aped, P.; Tartakovsky, E.; Fuchs, B. *Carbohydr. Res.* **1990**, *206*, 21. (b) Fuchs, B.; Schleifer, L.; Tartakovsky, E. *Nouv. J. Chim.* **1984**, *8*, 275.

[9] (a) Fuchs, B.; Auerbach, Y.; Sprecher, M. *Tetrahedron Lett.* **1972**, 2267. (b) Auerbach, Y. Ph.D. Thesis, Tel-Aviv University, 1973.

[10] (a) Allinger, N. L. *J. Am. Chem. Soc.* **1977**, *99*, 8127. (b) Allinger, N. L.; Chang, S. H. M.; Glaser, D. H.; Honig, H. *Isr. J. Chem.* **1980**, *20*, 5.

[11] Nørskov-Lauritsen, L.; Allinger, N. L. *J. Comput. Chem.* **1984**, *5*, 326.

[12] Binkley, J. S.; Frisch, M. J.; DeFrees, D. J.; Rahgavachari, K.; Whiteside, R. A.; Schlegel, H. B.; Fluder, E. M.; Pople, J. A. *GAUSSIAN 82*; Department of Chemistry, Carnegie-Mellon University: Pittsburgh, PA, 1982.

[13] Lee, H.; Wilmhurst, J. K. *Spectrochim. Acta* **1967**, *23A*, 347.

[14] Allen, F. H.; Bellard, S.; Brice, M. D.; Cartwright, B. A.; Doubleday, A.; Higgs, H.; Hummelink, T.; Hummelink-Peters, B. G.; Kennard, O.; Motherwell, W. D. S.; Rodgers, J. R.; Watson, D. G. *Acta Crystallogr.* **1979**, *35*, 2331.

[15] (a) Allen, F. H.; Kennard, O.; Taylor, R. *Acc. Chem. Res.* **1983**, *16*, 146. (b) Taylor, R.; Kennard, O. *Acta Crystallogr.* **1983**, *B39*, 517.

[16] (a) Lapasset, J.: Viani, R.; Bouab, O.; Lamaty, G.; Moreau, C. *Cryst. Struct. Commun.* **1980**, *9*, 1181. (b) Banyard, S. H.; Dunitz, J. D. *Acta Crystallogr., Sect. B* **1976**, *32*, 318. (c) Delaunay, J.; Simonet, J.; Toupet, L. *J. Chem. Soc., Chem. Commun.* **1986**, 1093. (d) Bandoli, G.; Nicolini, M. *J. Cryst. Spectrosc.* **1982**, *12*, 321.

[17] Our modification of MM2 for COCOC systems, namely, MM2-AE,[7] was used. The earlier version of the MM2 program (MM2-80)[10,11] had been obtained from the Quantum Chemistry Program Exchange (*QCPE* **1980**, *12*, 395), University of Indiana, Bloomington, IN 47401. A more recent, updated version (MM2-87) was also obtained from QCPE and reparametrized accordingly.

0002-7863/92/1514-5585$03.00/0

Table I. Relevant Structural Parameters of Five Independent (Out of Seven) Trimethyl Orthoformate Conformations[a]

	$g^-a;ag^+;g^-g^-$ 3-21G (MM2)	$aa;g^+g^+;g^-g^+$ 3-21G (MM2)	$g^-a;ag^-;g^-a$ 3-21G (MM2)	$g^-g^+;aa;ag^{+\,c}$ 3-21G (MM2)	$g^+g^-;g^-g^+;g^+g^{+\,c}$ 3-21G (MM2)
E_{rel}	0.00 (0.00)	1.80 (0.44)	3.19 (0.62)	9.16 (1.60)	4.77 (9.12)
L					
C1–O2	1.394 (1.394)	1.395 (1.396)	1.396 (1.402)	1.389 (1.398)	1.407 (1.402)
C1–O4	1.413 (1.410)	1.395 (1.396)	1.396 (1.402)	1.417 (1.414)	1.407 (1.402)
C1–O6	1.390 (1.399)	1.408 (1.411)	1.396 (1.402)	1.389 (1.403)	1.407 (1.402)
O2–C3	1.443 (1.445)	1.442 (1.445)	1.442 (1.443)	1.438 (1.445)	1.444 (1.442)
O4–C5	1.441 (1.440)	1.442 (1.445)	1.442 (1.443)	1.439 (1.440)	1.444 (1.442)
O6–C7	1.451 (1.445)	1.450 (1.441)	1.442 (1.443)	1.439 (1.441)	1.444 (1.442)
C1–H[b]	1.082 (1.117) [2]	1.082 (1.117) [2]	1.090 (1.117) [3]	1.089 (1.116)	1.074 (1.121) [0]
A					
O2–C1–O4	107.5 (108.1)	105.4 (106.7)	109.1 (106.5)	111.0 (107.7)	110.5 (115.0)
O2–C1–O6	109.5 (109.0)	111.8 (110.3)	109.1 (106.5)	105.2 (105.0)	110.6 (115.0)
O4–C1–O6	111.7 (109.9)	111.8 (110.4)	109.1 (106.5)	110.7 (107.9)	110.5 (115.0)
C3–O2–C1	116.3 (112.6)	114.9 (112.6)	116.2 (112.1)	116.3 (112.7)	119.5 (116.8)
C5–O4–C1	115.0 (112.3)	114.9 (112.6)	116.2 (112.1)	118.1 (112.4)	119.5 (116.8)
C7–O6–C1	116.0 (114.7)	115.6 (115.3)	116.2 (112.1)	116.2 (112.4)	119.5 (116.8)
D					
C3–O2–C1–O4	−54.5 (−89.4)	−171.8 (−153.2)	−52.7 (−88.3)	−52.7 (−106.1)	6.2 (36.2)
O2–C1–O4–C5	176.7 (152.1)	171.8 (153.6)	−171.8 (158.4)	120.2 (116.8)	−117.5 (−100.9)
C3–O2–C1–O6	175.9 (151.1)	66.5 (86.9)	−171.8 (158.3)	−172.5 (139.1)	−116.5 (−100.9)
O2–C1–O6–C7	49.4 (54.1)	58.9 (59.0)	−52.7 (−88.3)	173.7 (−163.3)	5.6 (36.2)
C5–O4–C1–O6	−63.2 (−89.0)	−66.5 (−86.5)	−52.7 (−88.2)	−123.2 (−130.3)	5.3 (36.2)
O4–C1–O6–C7	−69.5 (−64.2)	−58.9 (−58.6)	−171.8 (158.3)	53.6 (82.0)	−117.1 (−100.9)
C3–O2–C1–H	66.5 (33.0)	−50.2 (−33.9)	67.7 (35.0)	67.6 (19.5)	124.8 (147.7)
C5–O4–C1–H	54.5 (30.5)	50.2 (34.3)	67.7 (35.1)	−1.6 (−7.7)	124.0 (147.7)
C7–O6–C1–H	170.6 (173.9)	180.0 (−179.8)	67.7 (35.0)	−66.4 (−42.7)	124.2 (147.7)

[a] Cf. formula **3** and Figure 1. As calculated ab initio with the 3-21G basis set and by MM2-AE (results in parentheses): bond lengths (*L*, Å), bond angles (*A*, deg), and dihedral angles (*D*, deg). The headings represent idealized input geometries (cf. Figure 1) while the numerical values are output results. [b] Numbers in brackets give the number of lp's antiperiplanar to the CH bond in each conformer. [c] This high-energy conformer is presented here only to display its highly distorted final geometry.

(**3**), are shown in Figure 1, along with their relative energies as calculated ab initio, using GAUSSIAN 82 with the 3-21G basis set (and later also GAUSSIAN 90, to confirm minima and transition states) and MM2-AE[7,17] calculations. Relevant geometrical parameters of these calculated output structures are presented in Table I. It should be pointed out that an early infrared spectroscopic study in the vapor and solid phases and in solution, as well as a Raman study in the liquid,[13] led to the conclusion that trimethyl orthoformate assumes in the solid the $g^-a;ag^-;g^-a$ (C_3) conformation, but in solution it exists as a mixture of the $aa;g^+g^+;g^-g^-$ (C_s) and $g^-a;ag^+;g^-g^-$ conformations (cf. Figure 1). These three conformations are indeed calculated to be the most stable ones.

Clearly, the energies of the different conformers are governed by steric and anomeric interactions, and both computational methods yield a similar order of conformer stability, the ab initio energy differences being somewhat higher but the geometries being reasonably similar. Of the four high-energy forms, two converged to the lowest $g^-a;ag^+;g^-g^-$ form, while the two remaining forms show considerable discrepancy in their MO vs MM-calculated geometries (Table I) as well as energies. Indeed, these are not viable conformations (along with many others on this flexible system's potential surface) and deserve no further consideration in the present context. We include them, nevertheless, because they may occur in large, geometrically constrained molecules, as shown below.

Turning now to a closer scrutiny of the ab initio results, the following observations and rationalizations can be made:

1. Both $g^-g^-;ag^+;g^+g^-$ and $g^-g^+;ag^+;ag^-$ conformers converge to $g^-a;ag^+;g^-g^-$, the $g^-g^+;aa;ag^+$ conformer goes over into one with a highly distorted final geometry and high energy, and the unstable C_{3v} form $g^+g^-;g^-g^+;g^+g^-$ ends up with a C_3 final geometry (as can be deduced from their dihedral angles; cf. Table I), which is, moreover, not a thermodynamic minimum. Hence, only three viable conformers are left for a meaningful analysis.

2. Concerning the C–O and C–H bond lengths: (i) The inner C–O bonds are consistently shorter than the outer ones (see also below). (ii) The length of a C1–H bond increases as the number of lp's (lone pairs) antiperiplanar to it increases (cf. Table I), in line with the lp_O–σ^*_{C-H} anomeric interaction. (iii) In the $aa;g^+g^+;g^-g^-$ low-energy conformer, L(C1–O6) is larger than any of the other two, L(C1–O2) and L(C1–O4) (1.408 Å vs 1.395 Å, respectively). Since O6 participates in two *gg* anomeric units while O2 and O4 each participate in one *gg* and one *aa* anomeric

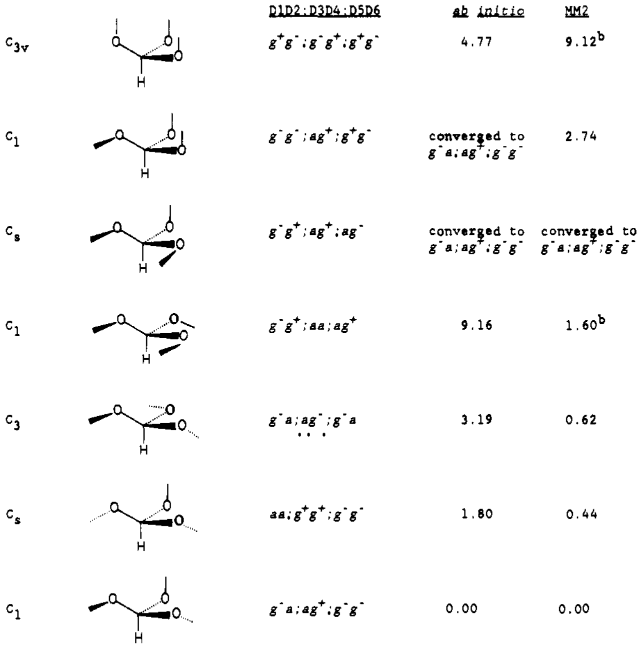

	Dihedral angles[a] D1D2:D3D4:D5D6	Relative Energies *ab initio*	 MM2
C_{3v}	$g^+g^-;g^-g^+;g^+g^-$	4.77	9.12[b]
C_1	$g^-g^-;ag^+;g^+g^-$	converged to $g^-a;ag^+;g^-g^-$	2.74
C_s	$g^-g^+;ag^+;ag^-$	converged to $g^-a;ag^+;g^-g^-$	converged to $g^-a;ag^+;g^-g^-$
C_1	$g^-g^+;aa;ag^+$	9.16	1.60[b]
C_3	$g^-a;ag^-;g^-a$	3.19	0.62
C_s	$aa;g^+g^+;g^-g^-$	1.80	0.44
C_1	$g^-a;ag^+;g^-g^-$	0.00	0.00

[a] conformers are defined through 3 pairs of dihedral angles as follows: D1–C3-O2-C1-O4; D2–O2-C1-O4-C5; D3–C3-O2-C1-O6; D4–O2-C1-O6-C7; D5–C5-O4-C1-O6; D6–O4-C1-O6-C7; g–gauche (synclinal); a–anti(periplanar).

[b] the MM2 optimized structure of this conformer differs considerably from the one calculated *ab initio*, hence, the energy difference discrepancy.

Figure 1. The seven independent, nondegenerate conformers (see note a) of trimethyl orthoformate (**3**). Relative energies as obtained from ab initio (3-21G) and MM2[7,17] calculations are given in kcal/mol.

Table II. Comparative X-ray (MM2-AE) Data for Selected Structural Parameters of the Orthoesters **5**–**8**[a]

	orthoester geometry[b]			
	$g^+g^-;g^-g^+;g^+g^-$ **5**	$g^-a;ag^-;g^-a$ **6**	$ag^-;g^+g^+;g^+g^-$ **7**	$ag^-;g^+g^+;g^+g^-$ **8**
L				
C1–O2	1.401 (1.402)	1.406 (1.406)	1.407 (1.421)	1.437 (1.406)
C1–O4	1.401 (1.402)	1.406 (1.406)	1.403 (1.385)	1.400 (1.396)
C1–O6	1.401 (1.402)	1.406 (1.406)	1.405 (1.397)	1.407 (1.405)
O2–C3	1.462 (1.442)	1.437 (1.443)	1.428 (1.436)	1.437 (1.441)
O4–C5	1.462 (1.442)	1.437 (1.443)	1.423 (1.449)	1.455 (1.457)
O6–C7	1.462 (1.442)	1.437 (1.443)	1.442 (1.443)	1.409 (1.441)
A				
O2–C1–O4	111.0 (111.2)	105.6 (105.6)	105.8 (107.1)	103.7 (107.3)
O2–C1–O6	111.0 (111.2)	106.1 (105.6)	111.2 (110.6)	108.7 (112.6)
O4–C1–O6	111.0 (111.2)	106.4 (105.6)	105.3 (105.4)	111.6 (107.7)
C1–O2–C3	111.0 (111.0)	113.9 (114.1)	115.6 (114.5)	116.9 (115.9)
C1–O4–C5	111.0 (111.0)	113.9 (114.1)	107.1 (108.2)	116.8 (116.2)
C1–O6–C7	111.0 (111.0)	113.9 (114.1)	108.1 (108.3)	112.2 (112.8)
D				
C3–O2–C1–O4	61.1 (62.3)	−65.4 (−65.7)	166.3 (−173.3)	−177.2 (−165.3)
O2–C1–O4–C5	−63.0 (−62.3)	−178.5 (−177.3)	−80.1 (−84.8)	−63.4 (−64.6)
C3–O2–C1–O6	−63.0 (−62.3)	−178.1 (−177.3)	52.4 (72.3)	63.9 (76.4)
O2–C1–O6–C7	61.1 (62.3)	−65.1 (−65.7)	80.1 (83.7)	47.5 (46.3)
C5–O4–C1–O6	61.0 (62.3)	−66.1 (−65.7)	37.7 (33.0)	53.4 (56.7)
O4–C1–O6–C7	−63.0 (−62.3)	−177.2 (−177.3)	−34.2 (−31.7)	−66.3 (−71.7)
C3–O2–C1–R	179.0 (180.0)	58.1 (58.4)	−72.6 (−52.8)	−57.9 (−47.9)
C5–O4–C1–R	179.0 (180.0)	57.9 (58.5)	157.1 (152.3)	173.7 (174.1)
C7–O6–C1–R	179.0 (180.0)	58.8 (58.5)	−153.6 (−149.8)	172.9 (172.5)

[a] See refs. 16a–d, respectively. Bond lengths (*L*, Å), bond angles (*A*, deg), and dihedral angles (*D*, deg). [b] See atom numbering in the orthoester moiety of each formula, to match the atom numbering in **3** (cf. also Figure 1).

unit, this can be understood as two bond shortenings and two bond elongations suffered by *L*(C1–O6) vs one bond shortening and one bond elongation suffered by both *L*(C1–O2) and *L*(C1–O4). One may recall that, within the structural manifestation of the anomeric effect, bond shortening is known to exceed the bond elongation effect.[11] Likewise, in the most stable $g^-a;ag^+;g^-g^-$ conformer (Figure 1), *L*(C1–O4) > *L*(C1–O2) ≃ *L*(C1–O6) (1.413, 1.394, and 1.390 Å), in accord with two bond elongations and one bond shortening for *L*(C1–O4), one bond shortening and one bond elongation for *L*(C1–O2), and one bond elongation and two bond shortenings for *L*(C1–O6).

3. Similar considerations may be applied to the C–O–C anomeric bond angles. In the $g^+g^-;g^-g^+;g^+g^-$ conformer, they are larger than in the $g^-a;ag^-;g^-a$ conformer (119.5° vs 116.2°, respectively), corresponding with the two anomeric interactions experienced by each oxygen atom in the former conformer vs one anomeric interaction in the latter.

As to the fit of the MM2 with the ab initio results (Table I), it is very good for the bond lengths and bond angles, but only moderately so for the dihedral angles. Taking into consideration, however, that the latter are the most sensitive conformational feature, especially in this exceedingly flexible molecule, the fit is satisfactory for the three viable (lowest energy) conformations. For the high-energy forms it expectedly fails, since the output geometries are considerably distorted from the initial, ideal forms, and each method seems to arrive at different structures in that region of the potential surface (e.g., the starting C_{3v} conformation is distorted into a high-energy C_3 form while it is taken ab initio to a peculiar saddle point).

Next, a group of 37 crystallographic structures, which include an orthoester moiety, was retrieved from the Cambridge Structural Database[14,15] (CSD; January 1990 version). Since most of those showed considerable deviations from the ideal conformations as well as severe geometrical constraints due to small or condensed ring systems, no statistical analysis was performed on their structural parameters. Instead, four least biased structures belonging to the $g^+g^-;g^-g^+;g^+g^-$ (**5**),[16a] $g^-a;ag^-;g^-a$ (**6**),[16b] and $ag^-;g^+g^+;g^+g^-$ (**7**, **8**)[16c,d] conformers were chosen for comparison of their structural parameters with the corresponding calculated ones, using MM2-AE.[7,17] The results are given in Table II and show good agreement between the observed and calculated data. It should be mentioned that the orthocarbonate problem has also been examined most recently.[19]

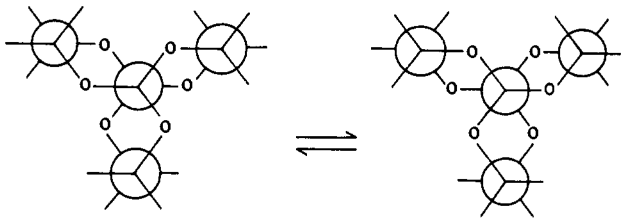

Figure 2. Inversion process of 2,5,7,10,11,14-hexaoxa[4.4.4]propellane (HOP) (**4**), in Newman projection.

In this context, a very interesting orthooxalate member of the group, namely, 2,5,7,10,11,14-hexaoxa[4.4.4]propellane (HOP, **4**), which we had prepared a long time ago,[9b] became the object of special scrutiny. The orthooxalate **4** was probed by two experimental techniques, in solution using NMR spectroscopy, and in the solid, using X-ray diffraction analysis, as well as by computation, using MM2-AE. The combined crystallographic and computational results for the most relevant structural parameters in HOP are given in Table III and show gratifyingly good agreement. The general crystallographic data are given in the Experimental Section, and the pertinent data from the X-ray diffraction analysis are assembled in Tables IV and V and depicted in Figure 3.

Critical examination of the structural data in Table III indicates a deceptive uniformity of, e.g., the internal C–O bond lengths in the COCOC units of **4**. This is obviously due to the overlap between the anomeric units in this double $g^-a;ag^-;g^-a$ system (cf. **4** and Figure 1). This overlap causes a peculiar cross-hyperconjugation which levels off the magnitude of the internal C–O bond lengths and the C–O–C bond angles. However, the internal C–O bond lengths are still outstandingly short, and the C–O–C bond angles are wide, indicating that the anomeric effect is fully operative, together with the intrinsic C–O bond shortening in the

---

(18) (a) The new MM3 program[18b,c] is also available from QCPE (public version). The official distributors are Technical Utilization Corporation, Inc., 235 Glen Village Court, Powell, OH 43065, and Tripos Associates, 1699 S. Hanley Road, St. Louis, MO 63144. (b) Allinger, N. L.; Yuh, Y. H.; Lii, J.-H. *J. Am. Chem. Soc.* **1989**, *111*, 8551 and subsequent articles, in particular that on alcohols and ethers.[18c] (c) Allinger, N. L.; Rahman, M.; Lii, J.-H. *J. Am. Chem. Soc.* **1990**, *112*, 8293.

(19) Narasimhamurthy, N.; Manohar, H.; Samuelson, A. G.; Chandrasekhar, J. *J. Am. Chem. Soc.* **1990**, *112*, 2937.

Table III. Observed vs Calculated Bond Lengths,[a] Bond Angles,[b] and Dihedral Angles[c] within the COCOC Moieties of HOP (4)

parameter	obsd, X-ray	calcd, MM2
L		
C1–O2	1.386	1.403
C1–O10	1.389	1.403
C1–O11	1.394	1.403
O2–C3	1.438	1.441
C4–O5	1.443	1.441
C6–O5	1.390	1.403
C6–O7	1.397	1.403
O7–C8	1.437	1.441
C9–O10	1.450	1.441
O11–C12	1.444	1.441
C13–O14	1.444	1.441
C6–O14	1.395	1.403
A		
C1–O2–C3	114.0	112.3
C4–O5–C6	112.7	112.4
O2–C1–O11	107.3	105.9
O2–C1–O10	107.1	105.9
O10–C1–O11	107.3	105.9
O5–C6–O14	107.5	105.9
O5–C6–O7	107.7	105.9
O7–C6–O14	107.0	105.9
C1–O10–C9	112.7	112.4
C6–O7–C8	113.5	112.3
C1–O11–C12	112.7	112.4
C6–O14–C13	113.5	112.4
D		
O2–C1–O10–C9	−68.8	−72.6
O2–C1–O11–C12	176.5	175.2
O10–C1–O2–C3	172.4	175.2
O10–C1–O11–C12	−68.6	−72.6
O10–C1–C6–O14	70.5	71.7
O10–C1–C6–O7	−49.1	−48.2
O10–C1–C6–O5	−169.5	−168.3
O10–C9–C8–O7	58.9	58.9
O11–C1–O2–C3	−72.6	−72.6
O11–C1–O10–C9	176.2	175.1

[a] *L* in Å. [b] *A* in deg. [c] *D* in deg.

Table IV. Atomic Coordinates and Thermal Parameters of HOP (4)

atom	x/a	y/b	z/c	U_{eq}[a]
C1	0.2878 (2)	−0.0316 (3)	0.7984 (2)	0.0283 (8)
O2	0.2578 (2)	−0.0286 (2)	0.6721 (1)	0.0329 (6)
C3	0.1239 (3)	−0.0014 (4)	0.6362 (2)	0.0397 (9)
C4	0.0436 (2)	−0.1356 (4)	0.6956 (2)	0.0418 (9)
O5	0.0708 (2)	−0.1276 (2)	0.8275 (1)	0.0367 (6)
C6	0.1993 (2)	−0.1579 (3)	0.8645 (2)	0.0288 (8)
O7	0.2255 (2)	−0.3347 (2)	0.8403 (2)	0.0372 (7)
C8	0.3589 (3)	−0.3794 (4)	0.8616 (3)	0.0433 (10)
C9	0.4369 (2)	−0.2636 (4)	0.7853 (2)	0.0394 (9)
O10	0.4156 (2)	−0.0813 (2)	0.8184 (2)	0.0344 (6)
O11	0.2782 (2)	0.1411 (2)	0.8408 (1)	0.0339 (5)
C12	0.2999 (3)	0.1543 (4)	0.9731 (2)	0.0426 (10)
C13	0.2034 (3)	0.0446 (4)	1.0310 (2)	0.0442 (10)
O14	0.2152 (2)	−0.1363 (2)	0.9920 (1)	0.0398 (6)

[a] U_{eq} is one-third of the trace of the orthogonalized U_{ij} tensor.

$C(OR)_3$ fragment, i.e., a carbon triply substituted with electronegative OR substituents.[20] Altogether, the related data of the calculated $g^-a;ag^-;g^-a$ conformer (Figure 1) and the observed and calculated data of **4** (Table III) and **6** (Table II) are in excellent agreement.

Table V. Bond Distances,[a] Bond Angles,[b] and Torsion Angles[b] of HOP (4)

	(a) Bond Distances		
C1–O2	1.386 (2)	C6–O7	1.397 (2)
C1–C6	1.551 (3)	C6–O14	1.395 (2)
O2–C3	1.438 (3)	C8–O7	1.437 (3)
C3–C4	1.501 (4)	O11–C12	1.444 (2)
C4–O5	1.443 (2)	C12–C13	1.489 (4)
O5–C6	1.390 (2)	C13–O14	1.444 (3)
C1–O10	1.389 (3)	O10–C9	1.450 (3)
C1–O11	1.394 (2)	C9–C8	1.498 (4)
	(b) Bond Angles		
O10–C1–O11	107.3 (2)	O5–C6–O7	107.7 (2)
C6–C1–O11	111.3 (2)	C1–C6–O14	111.4 (2)
C6–C1–O10	111.4 (2)	C1–C6–O7	111.7 (2)
O2–C1–O11	107.3 (2)	O7–C6–O14	107.0 (2)
O2–C1–O10	107.1 (2)	C1–O10–C9	112.7 (2)
O2–C1–C6	112.2 (2)	O10–C9–C8	108.5 (2)
C1–O2–C3	114.0 (2)	C9–C8–O7	109.9 (2)
O2–C3–C4	110.7 (2)	C6–O7–C8	113.5 (2)
C3–C4–O5	109.3 (2)	C1–O11–C12	112.7 (2)
C4–O5–C6	112.7 (2)	O11–C12–C13	109.2 (2)
C1–C6–O5	111.4 (2)	C12–C13–O14	109.1 (2)
O5–C6–O14	107.5 (2)	C6–O14–C13	113.5 (2)
	(c) Torsion Angles		
C1–O2–C3–C4	−54.6 (3)	O10–C1–O11–C12	−68.6 (2)
O2–C3–C4–O5	56.4 (3)	O2–C1–O11–C12	176.5 (2)
C3–C4–O5–C6	−58.5 (3)	C6–C1–O11–C12	53.5 (2)
O2–C1–O10–C9	−68.8 (2)	C4–O5–C6–O7	−68.6 (2)
C6–C1–O10–C9	54.2 (3)	C4–O5–C6–C1	54.2 (2)
O2–C1–C6–O7	71.0 (2)	C4–O5–C6–O14	176.5 (2)
O2–C1–C6–O14	−169.4 (2)	O5–C6–O14–C13	−70.2 (2)
O11–C1–C6–O5	70.8 (2)	C1–C6–O14–C13	52.1 (3)
O10–C1–C6–O5	−169.5 (2)	O5–C6–O7–C8	173.5 (2)
O2–C1–C6–O5	−49.4 (2)	C1–C6–O7–C8	50.9 (3)
C6–C1–O2–C3	49.9 (3)	O7–C6–O14–C13	174.3 (2)
O10–C1–O2–C3	172.4 (2)	O14–C6–O7–C8	−71.2 (3)
O11–C1–O2–C3	−72.6 (2)	C1–O10–C9–C8	−59.8 (3)
O10–C1–C6–O14	70.5 (2)	O10–C9–C8–O7	58.9 (3)
O10–C1–C6–O7	−49.1 (3)	C9–C8–O7–C6	−57.1 (3)
O11–C1–C6–O14	−49.2 (2)	C1–O11–C12–C13	−59.6 (3)
O11–C1–C6–O7	−168.8 (2)	O11–C12–C13–O14	59.2 (3)
O11–C1–O10–C9	176.2 (2)	C12–C13–O14–C6	−58.0 (3)

[a] In Å. [b] In deg.

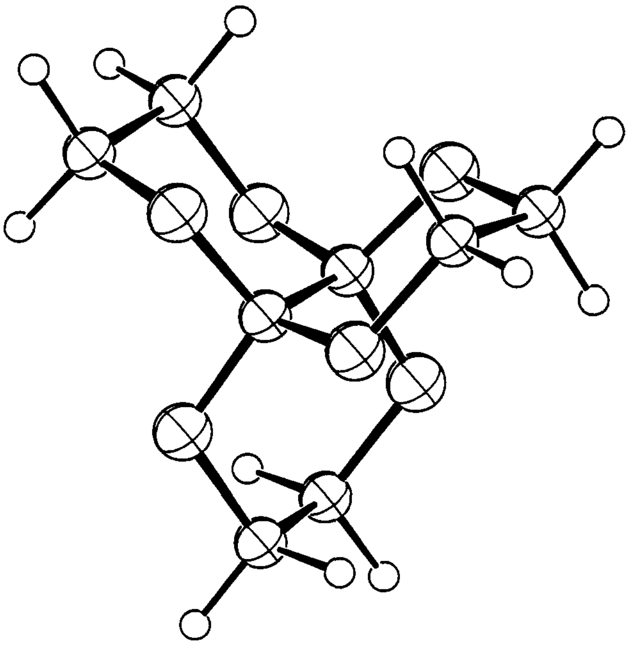

Figure 3. ORTEP drawing of the molecular structure of 2,5,7,10,11,14-hexaoxa[4.4.4]propellane (HOP) (**4**).

Another subject of considerable interest was the dynamic behavior of HOP (**4**), a D_3 molecule, occurring as two rapidly interconverting triple-chair enantiomers (Figure 2) at room temperature. Hence, its 12 protons are all isochronous and appear in its NMR spectrum as *one singlet* at 3.98 ppm. We had attempted to analyze the kinetics of inversion (racemization) in a variable temperature study of the CH_2–CH_2 moiety. To simplify the calculation at the time,[9] this AA′BB′ system was treated as a two-coupled-sites problem, to give an approximate result of $\Delta G^\ddagger$

---

(20) Allinger, N. L.; Imam, M. R.; Frierson, M. R.; Young, Y.; Schäfer, L. In *Mathematics and Computational Concepts in Chemistry*; Trinajstic, N., Ed.; Horwood: London, 1986; pp 8–17.

Table VI. Calculated (MM3) Dihedral Angles[a] of the Ground-State and Transition-State Conformations of HOP (**4**) on Its Ring Inversion Itinerary[b]

dihedral angle (*D*)	*ccc*	ts1 (*hc*)*cc*	(*tb*)*cc*	ts2 (*tb*)(*hc*)*c*	$(tb)_2c$	ts3 $(tb)_2(hc)$	$(tb)_3$	TS *bbb*
O2–C3–O4–O5	62.61	9.00	−69.66	−68.70	−68.06	−66.25	−66.15	0.00
C3–C4–O5–C6	−59.59	−49.56	38.85	39.40	33.74	34.99	34.03	−53.45
C4–O5–C6–C1	51.42	67.03	15.71	15.96	22.08	21.77	23.02	53.65
O5–C6–C1–O2	−47.00	−43.17	−46.71	−48.56	−51.10	−54.73	−55.35	0.00
C6–C1–O2–C3	51.42	3.35	15.71	18.62	16.65	23.11	23.02	−53.65
C1–O2–C3–C4	−59.59	13.42	38.84	36.33	39.32	33.86	34.03	53.45
C6–O7–C8–C9	−59.59	−59.01	−59.37	−45.93	39.32	34.07	34.03	−53.45
O7–C8–C9–O10	62.61	62.88	61.39	5.17	−68.06	−66.46	−66.15	0.00
C8–C9–O10–C1	−59.59	−60.09	−60.05	11.08	33.74	34.91	34.03	53.45
C9–O10–C1–C6	51.42	51.69	53.77	10.02	22.08	22.11	23.02	−53.65
O10–C1–C6–O7	−47.00	−46.72	−50.36	−49.51	−51.10	−54.56	−55.35	0.00
C1–C6–O7–C8	51.42	50.74	53.75	68.08	16.65	22.25	23.02	53.65
C1–O11–C12–C13	−59.59	−61.03	−59.37	−60.34	−59.62	−36.20	34.03	53.45
O11–C12–C13–O14	62.61	62.15	61.39	61.07	60.12	−2.59	−66.15	0.00
C12–C13–O14–C6	−59.59	−58.27	−60.05	−58.62	−59.62	10.13	34.03	−53.45
C13–O14–C6–C1	51.42	51.13	53.77	53.90	55.78	18.66	23.02	53.65
O14–C6–C1–O11	−47.00	−47.44	−50.36	−51.35	−53.37	−56.57	−55.35	0.00
C6–C1–O11–C12	51.42	52.73	53.75	54.63	55.78	65.62	23.02	−53.65

[a] *D* in deg. [b] Cf. Figure 4. Cf. formula 4 for atom numbering.

= 11.9 kcal/mol (the old result[9a] was 12.6, mainly due to a transmission coefficient of 1, which we revised now to $^1/_2$, vide infra).

We reinvestigated this problem by another approach,[21] namely, a variable temperature ^{1}H-NMR study of 2,5,7,10,11,14-hexaoxa[4.4.4]propellane-d_{11} (**4**-d_{11}), prepared from 2,2,3,3-tetrachlorodioxane and 1,2-dihydroxyethane-d_4, following our original procedure.[9] In the variable temperature NMR spectrum of HOP-d_{11} (**4**-d_{11}), the residual proton appears as a singlet at room temperature and is split at lower temperature into two singlets which coalesce at 30 °C. This was treated as an intramolecular exchange of two uncoupled sites: an axial and equatorial proton, with δ_{ae} = 28 Hz and T_c = 243 K. This gave $k_c = \pi\delta/2^{1/2} = 62$ s^{-1} and a value of ΔG^{*} = 11.8 kcal/mol, in very good agreement with the old value.

This free energy difference of activation for ring inversion of our 2,5,7,10,11,14-hexaoxa[4.4.4]propellane (**4**) should be compared with that of the carbocyclic analogue, i.e., [4.4.4]propellane (**4**, O = CH_2), or rather of its 3,3-difluoro derivative, which has been studied[22a] and exhibits a value of ΔG^{*} = 15.6 kcal/mol (recalculated at 243 K for this purpose). In its turn, this $\Delta\Delta G^{*}$ difference (15.6 − 11.8 = 3.8 kcal/mol) can be instructively compared with those of *cis*-decalin vs *cis*-1,4,5,8-tetraoxadecalin (**1**, X = H)[23,24] (12.8 − 9.8 = 3.0 kcal/mol) and of their 9,10-bis(bromomethyl) derivatives (X = CH_2Br) (14.7 − 11.7 = 3.0 kcal/mol).[2,22b] All these, when juxtaposed to the $\Delta\Delta G^{*}$ value for cyclohexane-1,4-dioxane (10.3 − 9.7 = 0.6 kcal/mol),[21b,c] show an interesting behavior, in that the monocyclic systems differ only slightly, but there is an appreciable increase of the energy difference in going from the mono- to the di- and tricyclic systems.

The question was now, in essence, what are the conformational stations (ground and transition states) on the ring inversion itinerary of HOP? We looked for an answer by calculating the minimum conformations of HOP and the corresponding transition states on the inversion path, using the MM3 force field[18] (which includes the parametrization for the anomeric effect). The driver option was used to sleuth after energy minima and, in particular, the transition states (where full matrix energy minimization gave one negative eigenvalue and an imaginary vibrational frequency).

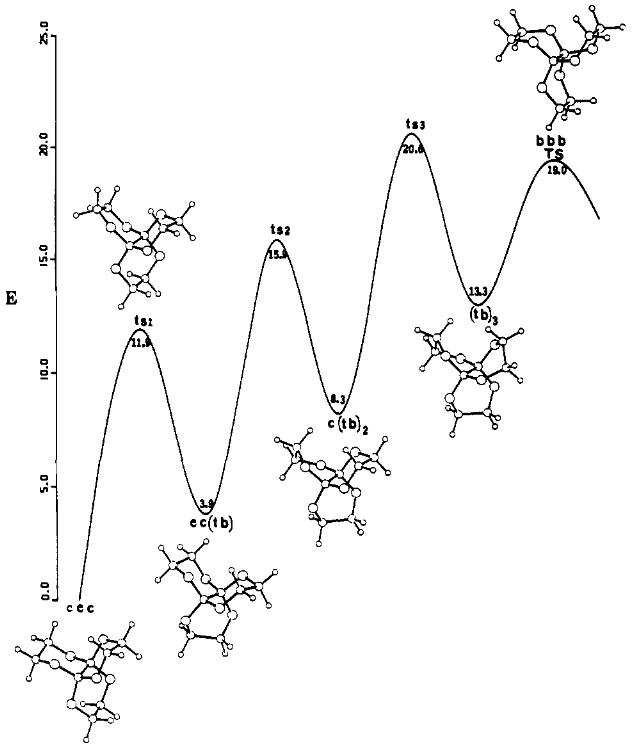

Figure 4. ORTEP drawings and the calculated (MM3) energy differences of transition state and minimum conformations of HOP (**4**), shown on its tentative ring inversion itinerary.

The results, namely, the relative energies and ORTEP drawings of the minima and transition states, are depicted on the potential curve in Figure 4, and the dihedral angles are given in Table VI. The global minimum is, of course, the triple-chair (*ccc*) form, which starts the inversion process by going to the next minimum, the twist-boat/double chair ((*tb*)*cc*),[29] through the first, half-

---

(21) (a) Anet, F. A. L.; Bourn, A. J. R. *J. Am. Chem. Soc.* **1967**, *89*, 760. (b) Anet, F. A. L.; Sandström, J. *Chem. Commun.* **1971**, 1558. (c) Jensen, F. R.; Neese, R. A. *J. Am. Chem. Soc.* **1971**, *93*, 6329; **1975**, *97*, 4345.

(22) (a) Gilboa, H.; Altman, J.; Loewenstein, A. *J. Am. Chem. Soc.* **1969**, *91*, 6062. (b) Altman, J.; Gilboa, H.; Ginsburg, D.; Loewenstein, A. *Tetrahedron Lett.* **1967**, 1329.

(23) Anet, F. A. L.; Anet, R. In *Dynamic NMR Spectroscopy*; Jackman, L. M., Cotton, F. A., Eds.; Academic Press: New York, 1975; Chapter 14, Tables VIII and X.

(24) Fraser, R. R.; Reyes-Zamora, C. *Can. J. Chem.* **1967**, *45*, 1012.

(25) Carothers, W. H.; Arvin, J. A.; Dorough, G. L. *J. Am. Chem. Soc.* **1930**, *52*, 3292.

(26) Sheldrick, G. M. In *Crystallographic Computing 3*; Sheldrick, G. M., Kruger, C., Goddard, R., Eds.; Oxford University Press: New York, 1985; pp 175–189.

(27) Sheldrick, G. M. *SHELX-76, Program for Crystal Structure Determination*; University of Cambridge: England, 1976.

(28) Senderowitz, H.; Golender, L.; Fuchs, B. Manuscript in preparation.

(29) There are actually more than one such conformation, with lower symmetry and of similar energy. We ignore them deliberately, for the sake of clarity and brevity.

chair/double chair ((*hc*)*cc*),[29] transition state. The third minimum, the double twist-boat/chair (($tb)_2c$),[29] is attained through the second transition state, the twist-boat/half-chair/chair ((*tb*)(*hc*)*c*).[29] The last, highest minimum is, as anticipated, the triple twist-boat (($(tb)_3$)).[29] It librates copiously but can consummate its twist-boat pseudorotation dynamics only by inverting its helicity (around the C1–C6 bond) through the fourth and last transition state, having the triple-boat (*bbb*) conformation.[30] From there on, the potential curve is the mirror image of that shown in Figure 4 with enantiomeric conformational ground and transition states, leading eventually to the inverted triple chair ($c^*c^*c^*$). The rate-determining step in the entire process appears to be represented by the third transition state, but the earlier two are very close and each requires ca. 12 kcal/mol. This is a rather high value compared with the above quoted literature values for 1,4-dioxane (9.7) and 1,4,5,8-tetraoxadecalin (9.8) as well as with our experimental *overall* ΔG^* value. It is difficult at this point to be more accurate, both because MM3 is currently not so well parametrized for the gauche effect[18c] and because we cannot assess accurately enough the solvent and entropy effects (the calculated energies are of enthalpic nature in the gas phase).

As to the central barrier (*bbb* transition state), it is well below the last barrier, and this justifies taking a transmission coefficient of $^1/_2$ in the evaluation of the ΔG^* value using the Eyring equation (vide supra). A more comprehensive treatment would have to include all the above mentioned carbocyclic analogues and some mixed analogues and is beyond the scope of this work. It will be, however, taken up in a forthcoming study.[28]

Experimental Section

2,5,7,10,11,14-Hexaoxa[4.4.4]propellane (HOP, 4) was prepared as reported previously[9] and recrystallized from ethyl ether. Its perdeuterated derivative, HOP-d_{12}, was analogously obtained from the reaction of ethylene glycol-d_4 (99% ^{2}H), first with oxalyl chloride to give 1,4-dioxane-2,3-dione-d_4.[25] The latter (570 mg), ethylene glycol-d_4 (1.2 g), and a catalytic amount of *p*-toluenesulfonic acid were dissolved in dry toluene and refluxed overnight with a Dean–Stark adapter. Evaporation of the solvent and chromatography on basic alumina (petroleum ether/chloroform 2:3) gave 35 mg of HOP-d_{12}, containing ca. 1% residual ^{1}H.

NMR spectra were taken on a Varian HA 100 spectrometer; chemical shifts are given in parts per million downfield from TMS and coupling constants in hertz. In the variable temperature ^{1}H-NMR spectrum of HOP-d_{11}, coalescence is observed at 243 K, and a chemical shift difference of 28 Hz was measured at 163 K and down.

Crystal Structure Analysis. X-ray diffraction data for HOP (**4**) were measured at ca. 20 °C on a CAD4 diffractometer equipped with a graphite monochromator, using Mo Kα ($\lambda = 0.7107$ Å) radiation and the ω scan technique with a scan range of $0.9 + \tan\theta°$. The cell constants and pertinent details of the experimental conditions are summarized below. Possible deterioration of the analyzed crystals was tested by frequently detecting the intensities of three standard reflections from different zones of the reciprocal space and was found negligible during the measurements. The data were not corrected for absorption or secondary extinction effects. A very strong reflection which appeared to suffer from extinction (2,0,0) was excluded from the final calculations.

The structure was solved by direct methods (SHELXS-86).[26] Its refinement was carried out by large-block least squares (SHELX-76),[27] including the positional and anisotropic thermal parameters of all the non-hydrogen atoms. The hydrogens were included in the structure factor computations in calculated positions and were assigned a fixed isotropic temperature factor of $U = 0.05$ Å^2. The final refinements were based only on those observations that satisfied the condition $F_o^2 > 3\sigma(F^2)$, using experimental weights [$w = \sigma^{-2}(F_o)$] and minimizing $w(\Delta F)^2$. They converged smoothly at relatively low discrepancy factors of $R = 0.04$. Final atomic coordinates of **4**, bond lengths, bond angles, and torsion angles are listed in Tables IV and V, and its ORTEP drawing is shown in Figure 3. The crystallographic atom-labeling scheme is that commonly used for propellanes, as shown in formula **4**.

Summary of Crystal Data and Experimental Parameters. $C_8H_{12}O_6$: M 204.18; space group $P2_1/c$; $Z = 4$; $a = 10.469$ (4) Å; $b = 7.578$ (4) Å; $c = 10.901$ (3) Å; $\beta = 94.85$ (3)°; $V = 861.7$ Å^3; $d_{\text{calcd}} = 1.574$ g cm^{-3}; $\mu = 1.28$ cm^{-1}; 2θ limits = 54°; scan rate = 3°/min; 1709 unique data > 0, 1099 data with $I > 3\sigma(I)$, $F(000) = 432$ e; $R = 0.041$; $R_w = 0.043$; $|\Delta\rho|_{\max} = 0.23$; "goodness of fit" = 1.15 e.

Acknowledgment. The calculations were performed on the IBM 3090 and CYBER 180/990E computers at the Computational Center of Tel-Aviv University, the staff of which provided valuable assistance. Dr. Larissa Golender's critical comments and assistance are gratefully acknowledged. This research has been supported by the Basic Research Fund of the Israel National Academy of Sciences.

Registry No. 3, 149-73-5; **4**, 37125-46-5; **5**, 27761-63-3; **6**, 7092-69-5; **7**, 141272-89-1; **8**, 141272-90-4.

Supplementary Material Available: Atomic coordinates of the hydrogen atoms of HOP (**4**) and anisotropic thermal parameters of the non-hydrogen atoms of HOP (**4**) (1 page). Ordering information is given on any current masthead page.

---

(30) There are also other, higher transition states for inversion which, however, need not be considered here.